Thermal Management of Next Generation Smartphones

Jeffrey Buyse
Graduate Student
Mechanical Engineering ASU FSE
Email: jbuyse@asu.edu

Ronnie Ramirez
Graduate Student
Mechanical Engineering ASU FSE
Email: reramir4@asu.edu

Sandeep Ramesh Moudgalya
Graduate Student
Mechanical Engineering, ASU-FSE
Email: smoudga1@asu.edu

Amm Hasib
Graduate Student
Mechanical Engineering ASU FSE
Email: ahasib@asu.edu

Abstract

As the modern technology of smart phones demands higher processing power beyond Moores law with the increased focus on graphic intense gaming and multi-tasking in a smaller device footprint, the design form factors need to be optimized in a way so that it can circumvent a manufacturer's biggest challenge—thermal management. One of the major bottlenecks of a smartphone is known as thermal throttling, which occurs to protect the processing chip from overheating and for ergonomic purposes. We proposed an innovative approach of both modifying the materials and design of heat spreaders as well as incorporating a composite metal fiber infused phase change system to reduce the thermal throttling probability as well as ensuring the smart phone skin temperature is lower than the ergonomic limit. Our models shows that we achieve an additional 20 minutes of work time at the maximum performance without throttling or surpassing the ergonomic skin temperature.

1 Introduction

To tackle the challenge of thermal management, most smartphone manufacturers currently utilize heat spreader systems or heat pipes to cool off the processor chip, which is the major heating element inside the device besides the battery. Most of the time copper is the material of choice as a heat spreader or heat sink because of its good thermal conductivity ($k = 385\frac{W}{mK}$), excellent solderability, and micro-electronic compatibility with other electronic components [1].

To achieve maximum heat transfer from the chip to the outside, an ideal device would have to have perfectly isothermal surfaces at the ergonomic temperature limit of 41°C. However, local hot spots are generated by the CPU and the lithium ion battery. This leads to inefficiencies in heat transport, which directly limits the maximum allowable power in the device. Wagner et. al. found that common commercially available portable devices are only 35-45% efficient at dissipating energy due to inhomogeneous surface temperatures or heat pockets, which leads to the need of spreading the heat in-plane. [2]

However, one shortcoming of using solely copper is its high density and specific cost, which create constraints to manage device space and weight limit in specification as well as increasing the manufacturing cost. Graphene or graphite sheets are then used as a mediator, which not only has good thermal conductivity (almost 2 to 4 times higher than copper), but also has a much lower specific density compared to copper. We also introduced PCM composite layers on top

of our sandwich layer heat spreader design so that excessive heat cannot penetrate through the plane after it passes from the heat spreader. Much of the heat spreaders duty is to dissipate the heat in-plane, but not through the plane. The goal of using a composite PCM with infused metal filaments is to overcome the low thermal conductivity of paraffin wax. Srilakshmi et al. found that the lower thermal conductivity of PCMs lead to slower thermal response of these systems and to alleviate the problem, he used metallic fillers and used a composite PCM based metal matrix structures to enhance the thermal conductivity of the composite. [3]

In our case, we thought of dispersing metal fillers in to our PCM making a composite material so that it can overcome the lower thermal conductivity of our PCM material.

2 Background

2.1 Current Thermal Management

The thermal management system in smartphones contributes to a very small portion of the manufacturing budget and most of it is dedicated to the IC, display, electromechanical features, battery, and camera.

This is interesting because when considering the root causes of chip failure, industrial investigation shows that around 55% of the chip failure is coming from the thermal issues.

One study shows that for every 2 °C rise in the chip temperature, the reliability of the chip decreased by 10%. [5] Due to this, thermal management in smartphones should be more of a concern and an innovative solution in this field may lead to higher reliability of the phones, which positively affects consumers and manufacturers.

2.2 Proposed Solution

Our approach towards this project was to consider a thermal management stack that would include a heat spreader and a phase change material (PCM). The heat spreader would be a stack of Cu-G-Cu and the PCM would be Paraffin 32-C. We decided to approach the project in three steps: (1) choose technology and design, (2) material selection, and (3) complete analytical and numerical models.

2.2.1 Design Selection

There were two key elements in choosing the right design selection. To void the potential heat pocket, we choose the heat spreader design and, in our study, literature we found that the more area of the heat spreader is, the far better is the in-plane heat transfer.

Another interesting observation from our research was even though that higher power is needed so even the largest heat spreader can not keep up with the increasing processing power and that heats up the phone surface. This forced us to choose an additional technology, which will be incorporated to the heat spreader design in order to dissipate more heat transfer.

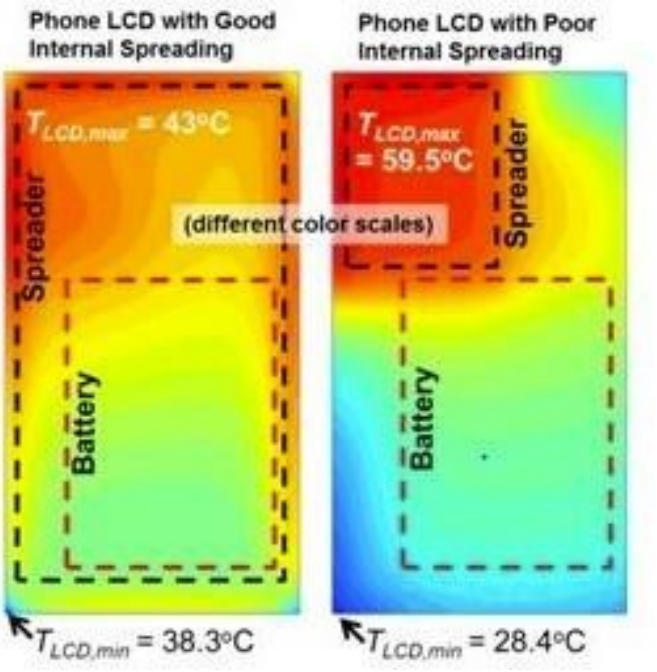

Fig. 1. Larger heat spreader reducing heat pocket

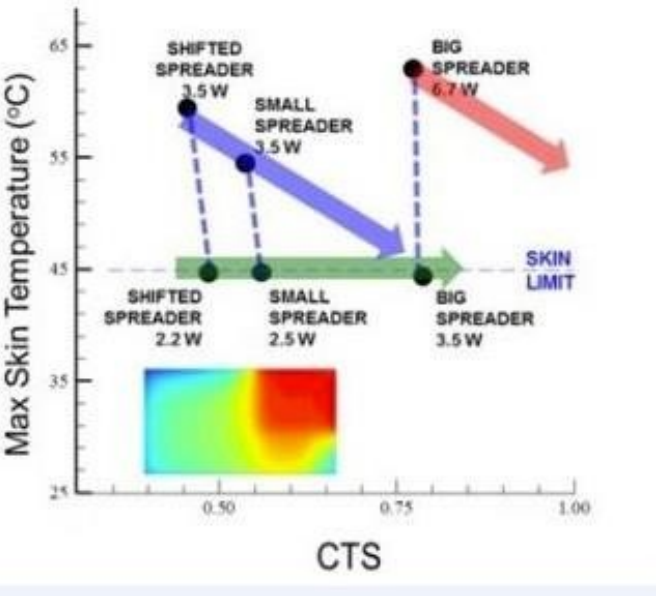

Fig. 2. Limitations of Large Heat Spreader

2.2.2 Materials Selection

The first decision was to select the materials for heat spreader. In order to compensate for the higher density effect and to minimize the space and weight, graphene layers have been used as a sandwich. Also, instead of using thermal insulation polymer, which adds more thermal resistance into the heat dissipation design, we can use Sn soldering for the bond with the lower level copper. It was found that 35 μm Cu-G-Cu sandwich was 8 °C lower than that on 50 μm Cu foil with the chip power of 1.4 W.

Our next step was to find the right PCM for the temperature range of our interest, which has high energy density or

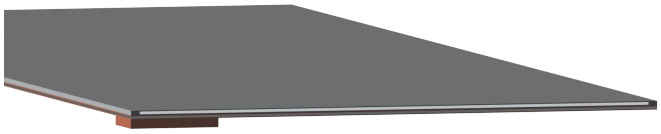

Fig. 3. 3D Model of Selected Design

heat of fusion and moderately high thermal conductivity. We found the best option leads to Paraffin 32-C (note: paraffin wax is flammable). Due to its flammable properties, we tried to find chlorinated paraffin wax, which is fire retardant. We also tried to increase the lower thermal conductivity of the paraffin wax, which is on the order of 72 $\frac{W}{mK}$, by dispersing Al or Graphene filaments to increase the thermal conductivity. This follows a law of diminishing returns so, we found a 10% mix of the metal particles will suffice resulting in the overall equivalent thermal conductivity to be 180 $\frac{W}{mK}$ for the PCM composites.

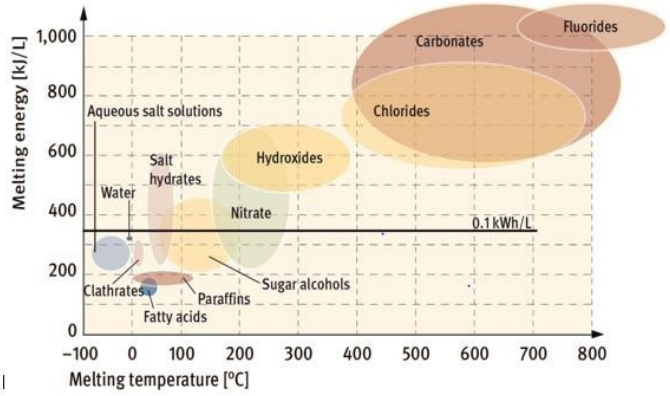

Fig. 4. PCM Selection

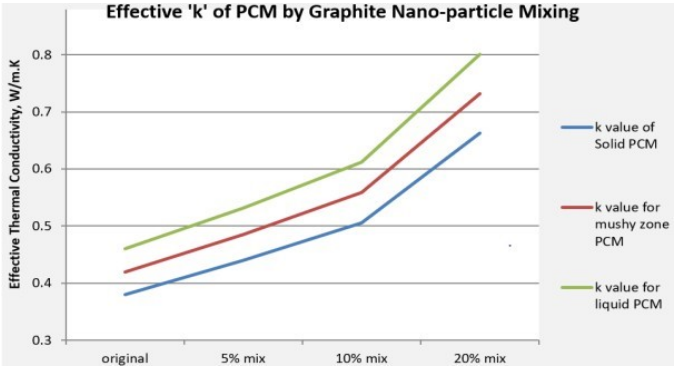

Fig. 5. Effective Thermal Conductivity of PCM

2.3 Governing Equations

Due to the smaller footprint of smartphones, forced convection is not a viable solution for heat dissipation. Due to this, in our analytical and numerical models, we mainly used heat conduction applying Fouriers law. Below are the governing equations used in the analytical and numerical models.

$$\overrightarrow{q} = -k\nabla T \tag{1}$$

$$q = hA(T_1 - T_2) \tag{2}$$

$$CTS = \frac{\theta_{ave}}{\theta_{max}} \tag{3}$$

$$R = \frac{\Delta T}{q} = \frac{L}{k} \tag{4}$$

$$C_{p,composite} = \frac{M_{Cu}}{M_{Cu}+M_{GS}} C_{p,Cu} + \frac{M_{GS}}{M_{Cu}+M_{GS}} C_{p,GS} \tag{5}$$

$$k_e = k_m \frac{2k_m + k_p - 2(k_m - k_p)f_p}{2k_m + k_p + (k_m - k_p)f_p} \tag{6}$$

$$\rho_{n-pcm} = \oslash_{np}\rho_{np} + (1 - \oslash_{np})\rho_{pcm} \tag{7}$$

$$\lambda\rho\left(\frac{ds(t)}{dt}\right) = k_s\left(\frac{\partial T_s}{\partial t}\right) - k_1\left(\frac{\partial T_1}{\partial t}\right) \tag{8}$$

$$k\frac{\partial^2 T}{\partial x^2} + \dot{q}_G = \rho c\frac{\partial T}{\partial t} = \frac{1}{\alpha}\frac{\partial T}{\partial t} \tag{9}$$

$$\nabla(k\nabla T) = \rho c\frac{\partial T}{\partial t} \tag{10}$$

$$R_{PCM} = \frac{1}{h_{c,o}APCM} \tag{11}$$

During the phase change period solid-liquid phase boundary shifts towards more liquid fraction (melting) or more solid fraction (solid) state depending on the latent heat absorbed or lost at the phase boundary, so tracking down the moving interface becomes critical. [7]

3 Experiment & Methodology

3.1 Analytical Model

In this analytical model we shall look at the extra time taken for the setup to reach throttling temperature with the PCM as opposed to without the PCM.

We assume that the CPU is generating heat at 2W while running at 5W capacity. The time taken for the PCM to heat up from idle temperature of 300K to throttling temperature at 343K.

The properties for Paraffin 32-Carbons are as follows:

Table 1. Properties of Paraffin 32-Carbons

Property	Value
Density (ρ)	1080 $\frac{kg}{m^3}$
Melting Point (T_m)	342.5 K
Specific Heat Capacity (C_p)	2700 $\frac{J}{kgK}$
Heat of Fusion (C_f)	200,000 $\frac{J}{kg}$
Dimensions of PCM (mm)	120 L x 60 W x Thickness

The time gained can be plotted against the mass of paraffin needed then a good balance between time savings and extra weight can be reached.

3.2 Numerical Model

The model used consists of a copper-graphite-copper heat spreader transferring heat from the chip to the PCM. The goal of using the PCM is to allow the processor to function at a maximum load for a longer period before throttling occurs. To explore the possibilities of using PCMs to increase time to throttling, a numerical method was constructed using the one-dimensional heat equation for the worst-case load. To construct the numerical solution, the Crank-Nicolson method was selected since it is unconditionally stable. The method is described in the following equation [8]:

$$-\beta T_{i-1}^{n+1} + (1+2\beta)T_i^{n+1} - \beta T_{i+1}^{n+1} = \beta T_{i-1}^{n} + (1-2\beta)T_i^{n} + \beta T_{i+1}^{n} \tag{12}$$

where,

$$\beta = \frac{\alpha \Delta t}{2\Delta x} \tag{13}$$

It is important to note that the beta values change depending on the material and depending on the temperature in the PCM. Due to a lack of access to variable properties for copper, graphite and PCMs, constant property assumptions were made. Properties in the PCM were altered to account for the melting temperature.

The Crank-Nicolson method forms a tridiagonal matrix which can be solved with elimination. The coefficients a, b and c are from the left-hand side of the equation and represent the next time level. The right-hand side of the equation is the d value and consists of the known values at the current time level. The default equations for a, b, c, and d are the following:

$$a = -\beta \tag{14}$$

$$b = 1 + 2\beta \tag{15}$$

$$c = -\beta \tag{16}$$

$$d = \beta T_{i-1}^{n} + (1-2\beta)T_i^{n} + \beta T_{i+1}^{n} \tag{17}$$

The equations for a, b, c, and d must be modified to account for the boundary and interface conditions. On the $x = 0$ boundary, a constant temperature was assumed, T_{chip}.

$$T(0,t) = T_{chip} \tag{18}$$

Because of this boundary condition, the d equation becomes:

$$d = \beta T_{i-1}^{n} + (1-2\beta)T_i^{n} + \beta T_{i+1}^{n} + \beta T_{chip} \tag{19}$$

On right boundary, assumed convective boundary condition with $T_{inf} = 25^{\circ}C$

$$-k\frac{\partial T(L,t)}{\partial x} = h(T_s - T_{inf}) \tag{20}$$

Because of this boundary condition, the b and d equations become:

$$b = 1 + 2\beta - \beta\left(\frac{k_{PCM}}{k_{PCM} + h_{conv}\Delta x}\right) \tag{21}$$

$$d = \beta T_{i-1}^{n} + (1-2\beta)T_i^{n} + \beta T_{i+1}^{n} + \beta T_{inf}\left(\frac{h_{conv}\Delta x}{k_{PCM} + h_{conv}\Delta x}\right) \tag{22}$$

At material interfaces for materials A and B there are the following interface boundary conditions [9].

$$T_A(x_{int},t) = T_B(x_{int},t) \tag{23}$$

$$-\frac{k_A(\partial T_A(x_{int},t))}{\partial x} = -\frac{k_B(\partial T_B(x_{int},t))}{\partial x} \tag{24}$$

The temperature condition is automatically enforced through the selection of a node-based mesh where the nodes fall on the material interfaces. Accounting for the derivative interface condition, the a and c equations at the interfaces become:

$$a = \frac{k_A(1+2\beta)}{k_A+k_B} - \beta \tag{25}$$

$$c = \frac{k_B(1+2\beta)}{k_A+k_B} - \beta \tag{26}$$

To assist with the convective boundary condition. The python CoolProps library is imported to account for the changing air properties at the convective boundary. Furthermore, it is assumed that only natural convection is occurring at the PCM boundary and that radiation is negligible. The goal of the numerical method used is to determine the amount of time to change the PCM from solid to liquid with the goal of optimizing the required PCM thickness.

4 Results & Discussion

4.1 Analytical Solution

The solution of the analytical model relied on varying the thickness of the phase change material. The thickness was varied on an order of mm at a time starting at 0.5 mm and increasing until a thickness of 1.5 mm was reached. Due to varying thickness, the results all relied on the thickness input. The time improvement before reaching the throttling temperature of 75 °C is apparent at a thicker phase change material with a time extension of 30 minutes at a 1.5 mm thick PCM. However, there is a balance of finding the right thickness for the PCM due to consumer wants of a thinner phone. There may be a slight trade off to have a bulkier phone that has a better thermal management system than a slim one. It is a matter of optimizing the time improvement versus the consumer needs.

From Figure 6, we can see that we get about a 20 minute time extension to work at maximum load with about a 1 mm thick PCM. This would mean around a 7.7 g weight increase or about a 4 % increase in weight.

Extrapolating this, one can assume that each percent of weight added to the phone, in terms of a PCM, will yield a 5 minute time extension at maximum performance.

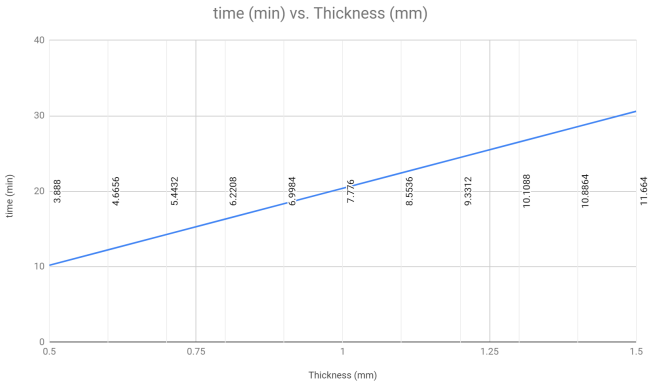

Fig. 6. Time saved vs. thickness added to device

4.2 Numerical Solution

The numerical solution described is not functioning due to a failure to account for heat into the system or heat generated within the system. As a result, the temperatures drop instead of increase. To correct the issue, the x=0 boundary condition was changed from a constant temperature condition to a constant flux condition to account for the heat coming into the heat spreader system from the chip. The maximum chip power and the area of the chip were used to calculate the constant flux into the x = 0 boundary. Because of this change, the temperatures no longer decrease; however, they appear to approach steady state very rapidly which was not expected. Furthermore, there appears to be a discontinuity at one of the interfaces indicating that an error was made defining the interface. The team is not confident in the current numerical solution and recommends further research into modeling PCMs with a finite difference method as well as consulting experienced experts in PCM research.

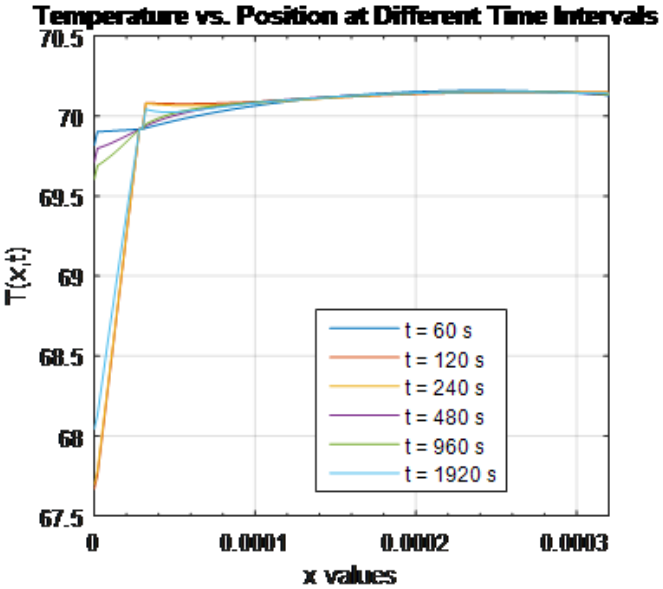

Fig. 7. Temperature vs. Position at Different Time Intervals

Figure 7 is the result of the program after changing the $x = 0$ boundary condition to a constant flux condition. This ended up being a different approach than first assumed in the initial numerical modeling stage; however, the change was made in order to produce a result.

5 Conclusion

Our analytical model determined that with a 1 mm thick PCM in our thermal management stack, one could expect to gain an additional 20 minutes of work time at maximum performance before one would experience throttling. We also saw that at a maximum thickness of 1.5 mm for the PCM, one could expect upwards of 30 minutes of work time at maximum performance before throttling.

Unfortunately, the numerical model is a very difficult project to tackle and it did not produce the results we were hoping for; however, it is a framework to further pursue in order to produce results more in line with expectations.

Overall, the experiment was positive and in line with the original expected benefit of performing better than current thermal management systems in smartphones. There is more work to be done to further prove its efficacy; however, as a proof of concept, it stands to allow one to see the benefits of the system through both increased work time before throttling at maximum performance and also through its capability to keep phone temperatures at a lower ergonomic skin temperature.

6 Future Work

The system is not as optimized as it could be and thus, some future work could be done to further improve the system. One main source of improvement would be to further analyze the system analytically. Our current analysis, while showing some decent results, is not as thorough as it could be. There are many more factors to look at in terms of the heat transfer through, not only the heat spreader, but as well as the PCM. Phase change materials are a very difficult thing to analyze analytically as well as numerically. Similarly, our numerical model had a few bugs that did not allow it to run as smoothly as well as not produce the expected results. Thermal management is a neglected subject in terms of smartphones, but the potential is there, from our models, to make it even better than it currently is. It may be that thermal management follows the law of diminishing returns and does not provide much benefit past what is currently available. However, we have shown that there is potential in using phase change materials in a smartphone as part of a thermal management stack along with a heat spreader. This is not an open-and-closed situation—there is much more here to be explored.

7 References

[1] B. Jiang, H. Wang, G. Wen, E. Wang, X. Fang, G. Liu, and W. Zhou, Coppergraphitecopper sandwich: superior heat spreader with excellent heat-dissipation ability and good weldability, The Royal Society of Chemistry, 07-Mar-2016. [Online]. Available: https://pubs.rsc.org/en/content/articlelanding/2016/ra/c6ra00057f#!divAbstract. [Accessed: 25-Apr-2019].

[2] A. Vodnick, Development and Application of Thermally Functionalized Structural Materials for Heat Spreading in Handheld Devices, Materion. [Online]. Available: https://materion.com/-/media/files/technicalmaterials/technical-papers/mtm-technical-paper-38.pdf?la=enhash=D49F475DCA9306808B4AA98DBC97C156. [Accessed: 25-Apr-19AD].

[3] S. Lingamneni, A parametric study of Microporous Metal Matrix-Phase Change Material composite heat spreaders for transient thermal applications, A parametric study of Microporous Metal Matrix-Phase Change Material composite heat spreaders for transient thermal applications - IEEE Conference Publication, 27-May-2014. [Online]. Available: https://ieeexplore.ieee.org/document/6892372. [Accessed: 25-Apr-2019].

[4] E. Barbarini, Thermal Management in Smartphones: Technology Comparison 2017, SystemPlus Consulting, Nov-2017. [Online]. Available: https://www.systemplus.fr/wp-content/uploads/2017/11/SP17369_thermal_management_smartphone_overview_System_sample.pdf. [Accessed: 25-Apr-2019].

[5] A. Kalyan, Heat Transfer Enhancement in a Smart Phone, ResearchGate, Apr-2017. [Online]. Available: https://www.researchgate.net/publication/316537100_Heat_Transfer_Enhancement_in_a_Smart_Phone. [Accessed: 25-Apr-2019].

[6] Zalba, B., Marin, J.M., Cabeza, L.F., Mehling, H. quot;Review on thermal energy storage with phase change : materials, heat transfer analysis and applications.quot; Applied Thermal Engineering 23 (2003): 251-283.

[7] Sharma, A., Tyagi, V.V., Chen, C.R., Buddhi, D. quot;Review on thermal energy storage with phase change materials and applications.quot; Renewable and Sustainable Energy Reviews 13 (2009): 318-345.

[8] Hoffman, K. A. and Chiang, S. T., 2000, Computational Fluid Dynamics Volume 1, 4th ed., Engineering Education System, Wichita, KS, Chap 3.

[9] Cengel, Y. A. and Ghajar, A. J., 2011, Heat and Mass Transfer: Fundamentals & Applications, 4th ed., McGraw-Hill, New York, NY, Chap 2.

8 Appendix A: Sample Code

```
Tm = 75; % degC %melting temperature of parafin wax
Tinf = 25;% degC ambient air temp inside of phone

%alpha = k/(rho*cp)
alphaCu = kCu/(rhoCu*cpCu);
alphaGr = kGr/(rhoGr*cpGr);
alphaPCMl = kPCMl/(rhoPCMl*cpPCMl);
alphaPCMs = kPCMs/(rhoPCMs*cpPCMs);

dtMax = 0.01; %unconditionally stable.  any dt is valid
Tinit(1:P) = 25; %Initial T condition
outputTime = [0.1 inf]; %given output times
z = 1; %flag variable

time = 0; %define start time
endTime = outputTime(end-1)+dtMax;
Tn = Tinit; %set Tn vector to initial condition

%hconv
g = 9.81; %m/s^2
Lc = ((60*120)/(2*60+2*120))*10^-3;%m
%{
Tf =(Tn(end)+Tinf)/2+273.15;
betaAir = 1/(Tf+273.15);
muAir = PropsSI('V','T',Tf,'P',101325,'Air');
rhoAir = PropsSI('D','T',Tf,'P',101325,'Air');
nuAir = muAir/rhoAir;
PrAir = PropsSI('PRANDTL','T',Tf,'P',101325,'Air');
kAir = PropsSI('L','T',Tf,'P',101325,'Air');

Ra = (g*betaAir*(Tn(end)-Tinf)*Lc^3)/nuAir^2*PrAir;
if Ra >=10^4 && Ra <=10^7
    Nu = 0.54*Ra^(1/4);
end
if Ra >=10^7 && Ra <=10^11
    Nu = 0.15*Ra^(1/3);
end
hconv = kAir/Lc*Nu;
%}
hconv = 0;
Tchip = 70;
Tn(1) = Tchip; %x = 0 BC.  Throttling temp
%Tn(end) = (kPCMs/(hconv*dx)*Tnl(end-1)+Tinf)/2; %x = 2 BC.  Convective BC
%ignored because Ts = Tinf
Beta = zeros(1,P-2);%preallocate Beta
eps = 10^-12;
while time <= endTime

    dt = dtMax; %initialize dt to max step

    zplot = 0; %plot variable set to off
    if (time < outputTime(z)) && (time + dt >= outputTime(z))
        dt = outputTime(z) - time; %setFlagforOuput;
        z = z+1; %increment z if plot time hit;
        zplot = 1; %toggle data storage on
    end
```

Fig. 8. Sample Code of Numerical Model